



Published in final edited form as:

Nat Biotechnol. 2019 October ; 37(10): 1131–1136. doi:10.1038/s41587-019-0223-y.

Supercooling extends preservation time of human livers

Reinier J. de Vries^{1,2,3}, Shannon N. Tessier^{1,3}, Peony D. Banik^{1,3}, Sonal Nagpal^{1,3},
Stephanie E.J. Cronin^{1,3}, Sinan Ozer^{1,3}, Ehab O.A. Hafiz^{1,3,4}, Thomas M. van Gulik², Martin
L. Yarmush^{1,3}, James F. Markmann^{1,5}, Mehmet Toner^{1,3}, Heidi Yeh^{1,5}, Korkut Uygun^{1,3}

¹Center for Engineering in Medicine, Harvard Medical School & Massachusetts General Hospital, Boston, Massachusetts, United States. ²Department of Surgery, University of Amsterdam, Amsterdam, the Netherlands. ³Shriners Hospital for Children, Boston, Massachusetts, United States. ⁴Department of Electron Microscopy Research, Theodor Bilharz Research Institute, Giza, Egypt. ⁵Center for Transplant Sciences, Massachusetts General Hospital, Boston, Massachusetts, United States

Abstract

The inability to preserve vascular organs beyond several hours contributes to the scarcity of organs for transplantation^{1,2}. Standard hypothermic preservation at +4°C^{1,3} limits liver preservation to less than 12 hours. Our group previously showed that supercooled ice free storage at –6°C can extend viable preservation of rat livers^{4,5}. However, scaling supercooling preservation to human organs is intrinsically limited because of volume-dependent stochastic ice formation. Here, we describe an improved supercooling protocol that averts freezing of human livers by minimizing favourable sites of ice nucleation and homogeneous preconditioning with protective agents during machine perfusion. We show that human livers can be stored at –4°C with supercooling followed by subnormothermic machine perfusion, effectively extending the *ex vivo* life of the organ by 27 hours. We show that viability of livers before and after supercooling is unchanged, and that after supercooling livers can withstand the stress of simulated transplantation by *ex vivo* normothermic reperfusion with blood.

The absence of technology to preserve organs for more than a few hours is one of the fundamental causes of the donor organ shortage crisis^{1–3}. Subzero preservation has the potential to extend the organ storage limits^{1–5}, as the metabolic rate halves for every 10°C

Users may view, print, copy, and download text and data-mine the content in such documents, for the purposes of academic research, subject always to the full Conditions of use:http://www.nature.com/authors/editorial_policies/license.html#terms

Correspondence and requests for materials should be addressed to kuygun@mgh.harvard.edu.

Present address: 51 Blossom Street, Boston, Massachusetts, 02114

Author contributions

R.J.V., S.N.T. and K.U. conceived and designed the study; R.J.V., P.B., S.N., S.C. and S.O. performed data acquisition; R.J.V., S.N.T., E.O.A.H., H.Y., M.L.Y., J.F.M., M.T., and K.U. analyzed and interpreted data; R.J.V., S.N.T. and S.O. designed and constructed the perfusion and supercooling system; R.J.V., S.N.T. and K.U. wrote the manuscript; R.J.V., S.N.T., E.O.A.H., T.M.G., M.L.Y., J.F.M., M.T., H.Y. and K.U. participated in critical revision of the manuscript for intellectual content; R.J.V., S.N.T. and K.U. performed statistical analysis. All authors contributed to the preparation of the manuscript.

The authors declare competing financial interests. Drs. Toner, Yarmush, de Vries, Uygun and Tessier have provisional patent applications relevant to this study. Dr. Uygun has a financial interest in Organ Solutions, a company focused on developing organ preservation technology. Author's interests are managed by the MGH and Partners HealthCare in accordance with their conflict of interest policies.

reduction in temperature⁴ thereby reducing organ deterioration rate. Supercooling has the major advantage that it allows preservation at high subzero storage temperatures, while avoiding phase transitions and consequent lethal ice-mediated injury³⁻⁵, as well as toxicity of most common cryopreservatives. However, human livers are about 200 times larger than rat livers, which exponentially increases the likelihood of heterogeneous ice nucleation during supercooling, a stochastic process that is dependent on volume and temperature⁶. Indeed, repeating the protocol we previously employed to supercool rat livers led to freezing of the livers (Supplementary Fig. 1).

We took a three-pronged approach to eliminate freezing of the livers during subzero storage. First and most critically, we minimized air liquid interfaces, that are thermodynamically favourable sites of heterogenous ice nucleation due to surface tension. Our Center (Center for Engineering in Medicine, Harvard Medical School & Massachusetts General Hospital, Boston MA, USA) has previously shown that by eliminating the storage media-air interface by sealing with an immiscible phase, heterogenous ice nucleation can be eliminated and up to 100 ml media can be stored at -20°C stably for up to 100 days⁶. While the presence of a human liver prevents the use of the same approach with the same efficacy, we minimized liquid air interfaces by de-airing the storage solution bag ahead of supercooling to minimize such obvious ice nucleation (see Online Methods).

Second, we tested the addition of protective agents to depress the melting point of the livers, which meant reducing the degree of supercooling. The standard clinical hypothermic preservation (HP) solution is University of Wisconsin solution (UW), which we used as the base for our supercooling preservation solution. UW contains hydroxyethyl starch, raffinose and potassium lactobionate that could modify ice nucleation and lower the melting point as compared to pure water (Supplementary Table 1). Potential toxicity of additional cryoprotective agents during prolonged high subzero preservation is an important consideration, which is why we had avoided them in our prior rat studies. Informed by our prior work (see Online Methods) and literature, we chose two additives that are popular in cryopreservation but are not used in hypothermic organ preservation: 1) Trehalose, for the protection of the extracellular compartment and to provide cell membrane stabilization at subzero temperatures⁷, in addition to PEG⁸ which was already present in our rat protocol. 2) Glycerol, which is freely permeable over plasma membranes⁷ and therefore supplements 3-OMG which accumulates intracellularly⁴ and was a key additive for rat livers. Although glycerol is common in cryopreservation, the latest reports date back to the 70s and it has not been used for hypothermic or high subzero organ preservation in modern history⁹.

Third was the loading scheme of the new preservation cocktail. Although the melting point of the preservation solution was depressed by the addition of trehalose and to a greater extent by glycerol (Supplementary Table 1), the solution melting point does not fully reflect the melting point depression of the actual livers when loaded with that solution. The melting point of the preconditioned livers (Supplementary Fig. 2) was significantly ($p < 0.0001$, $t(13) = 7.761$) higher (-2.1°C) as compared to the preservation solution (-3.03°C), which can potentially be explained by incomplete equilibration and a dilution effect of the preservation solution in the relatively large organ volume. While a 10 g rat liver can be simply flushed manually with a syringe, we experienced that the increased size of human grafts makes

homogeneous loading of protective agents substantially harder, which initially resulted in freezing of the grafts. Uniform distribution of protective agents within the tissue is crucial in supercooled storage, since ice might initially nucleate at an insufficiently protected site and propagate through the entire organ. Also, the increased viscosity of the preservation solution due to the additional protective agents could potentially increase shear stress on the endothelium. The excessive shear stress can consequently cause substantial endothelial injury¹⁰. To address both concerns, we introduced an additional hypothermic machine perfusion (HMP) step to homogeneously precondition the organs and avert freezing during supercooling. Briefly, the liver was machine perfused at +4°C, without recycling of the preservation media. The preservative agent concentrations were increased gradually during HMP to avoid potential osmotic injury, and the perfusion flowrates and pressures were accurately compensated to account for the increase viscosity and avert endothelial injury.

Because subnormothermic machine perfusion (SNMP) after supercooling was critical for transplant survival in rats, we also chose this modality to recover the human livers after supercooling. Additional modifications related to engineering of the system to allow perfusion of human livers at multiple temperatures and in different configurations finally resulted in the human liver supercooling protocol that is outlined in Figure 1 and described in detail in the Online Methods and Supplementary Figure 3.

To assess if supercooled human livers retained their viability, we took advantage of the fact that SNMP has been shown to allow detailed *ex vivo* assessment of liver viability^{4,11–13}. To be able to control for donor-to-donor variability in the marginal human livers that were rejected for transplantation (Supplementary Table 2), we compared viability parameters during SNMP before, and after supercooling (Fig. 2). Adenylate energy content, and particularly, the organs' ability to recover it during (re)perfusion is considered the most representative metric for liver viability^{3,12,14–16}. The energy charge was low at the start of SNMP both before (i.e. directly after HP) and after supercooling due to slowly ongoing vital cell processes during storage. In this regard, the glycerol in the supercooling preservation solution was potentially phosphorylated at expense of ATP and ADP, contributing to the energy charge reduction during supercooling. Nonetheless, no statistical difference between pre- and post-supercooling energy charge was found (Fig. 2a and Supplementary Fig. 4a and b). Importantly, the energy charge recovered significantly during SNMP ($p < 0.0001$, $F(1, 4) = 443.9$) both before and after supercooling ($p = 0.0209$, mean diff. (95% CI) = 0.190 (0.043 to 0.336), $\eta^2 = 0.75$ and $p = 0.0185$, mean diff. (95% CI) = 0.197 (0.050 to 0.343), $\eta^2 = 0.47$, respectively). The mean difference in end-SNMP energy charge was smaller than 20%. By comparison, >40% differences are observed in adenylate energy content between successful and unsuccessful transplanted livers in both large animal¹⁵ and clinical^{16–18} studies.

Additional important viability parameters during SNMP include bile production, vascular resistance and oxygen uptake, which were significantly correlated to transplant survival after supercooling in rats⁴. Of these parameters, bile production has been clinically correlated to graft function after liver transplantation¹⁸ and to human liver function during SNMP¹². No statistical significance was found in bile production ($p = 0.433$, $F(1, 4) = 0.759$). Three livers produced the same amount of bile during SNMP before and after supercooling (Fig.

2b), indicating successful preservation. One liver (liver 2) did not produce bile either before or after supercooling and one liver (liver 1) stopped bile production after supercooling, while other viability parameters in both indicated preserved viability. Portal and arterial resistances (Fig. 2c) after supercooling were stable and no significant differences were found compared to pre-supercooling SNMP ($p = 0.649$, $F(1, 4) = 0.241$, and $p = 0.809$, $F(1, 4) = 0.067$, respectively). The maximal observed mean difference between portal vein resistance before and after supercooling was 21% (at $T = 90$ min), while much higher 100%–150% increases are reported in literature for non-viable livers^{4,19}. The recovery in oxygen uptake rate at the start of SNMP was the same before and after supercooling. Although the oxygen uptake at the end of SNMP was higher before supercooling, the difference in oxygen uptake rate at individual timepoints did not reach statistical significance ($p = 0.272$, $F(1, 4) = 1.617$). To account for the initial recovery phase of oxygen uptake during the first two hours of SNMP – which might attenuate a potential difference in the oxygen uptake at the end of perfusion – we also compared the oxygen uptake at the end of perfusion (area under the curve (AUC) at $T = 120$ min), which did not show a statistically significant difference ($p = 0.233$, $t(8) = 1.292$). The mean difference in total oxygen uptake (total AUC) before and after supercooling (Fig. 2d) was 17% and three times lower than the reported 51% reduction in oxygen uptake (AUC) during SNMP of human livers with impaired viability¹¹.

Similar to bile production, lactate clearance is an important liver function which was observed both before and after supercooling (Supplementary Fig. 4c). Moreover, we found significantly higher lactate levels before supercooling ($p = 0.0105$, $F(5, 20) = 4.056$) that prevailed during the first hour of SNMP as compared to post-supercooling ($p = 0.0044$, mean diff. (95% CI) = 2.714 (0.727 to 4.701) $\eta^2 = 0.42$ at $T = 30$ min and $p = 0.0164$, mean diff. (95% CI) = 2.326 (0.339 to 4.313), $\eta^2 = 0.17$ at $T = 60$ min). (Supplementary Fig. 4d). Since the livers were transported to our hospital under hypothermic preservation (HP) conditions, we hypothesize that the build-up of lactate during HP is higher, compared to supercooling due to deeper metabolic stasis. As we observed this same pronounced trend in the DBD liver (liver 4), this is unlikely to be solely due to warm ischemia during procurement of DCD livers.

In addition to liver function and metabolism, we assessed liver injury before and after supercooling. Hepatocellular injury was the same and stable before and after supercooling as demonstrated by aspartate aminotransferase (AST), alanine aminotransferase (ALT) (Fig. 2e) and potassium (Supplementary Fig. 4e) concentrations in the perfusate. The transaminase levels we found are low compared to others^{11,12,20–22}, which could be explained by the two liter perfusate that was non recirculated at the beginning of SNMP to wash out the protective agents. The stability of transaminase levels during perfusion is of particular importance since it confirms absence of potential toxicity of the protective agents. This is confirmed by histology (Fig. 2f–g) which shows preserved lobular architecture with viable hepatocytes and intact sinusoidal endothelial cells. No necrosis, nor substantial increase in apoptotic cells was observed (Fig. 2h) and preexisting focal signs of hepatocellular and endothelial injury marginally aggravated during preservation. In summary, we find that the human livers tested displayed no substantial difference in viability before and after extended subzero supercooling preservation. Although the difference in energy charge, oxygen uptake and apoptosis were not significant and small compared to

referenced literature, they should be further investigated aiming to improve supercooling preservation.

With initial success of our supercooling protocol, we then subjected three livers to additional *ex vivo* normothermic reperfusion with blood as a model for transplantation^{16,23} (Fig. 1e and 3). Unlike normothermic machine perfusion (NMP) which is intended to assess and improve liver viability, the blood used in reperfusion studies contains white blood cells (WBC), platelet and complement which are key components of ischemia reperfusion injury. This fundamental difference should be taken into account when we compare the viability parameters during reperfusion after supercooling to NMP data in literature after hypothermic preservation, which does not include the immunologic components. Accessibility of whole blood in sufficient quantities for human liver reperfusion studies is severely limited. Therefore, we recombined red blood cells and fresh frozen plasma instead. Although this is suboptimal to the use of fresh whole blood, we specifically used non-leuko reduced blood products and confirmed the presence of white blood cells and platelets (Supplementary Table 3).

During blood reperfusion the livers had a stable energy charge (Fig. 3a and Supplementary Fig. 5a and b). Moreover, the mean energy charge was higher after just 7 hours of HP than we previously found in both *ex vivo* studies and directly after reperfusion in transplanted human livers¹⁶. The stability of energy charge during reperfusion is of additional importance since a drop after initial restoration of energy charge during clinical reperfusion was significantly correlated with early allograft dysfunction¹⁶. This could potentially be explained by mitochondrial function that cannot keep up with the increased energy demand after the transition from a reduced to a full metabolic rate during normothermic reperfusion. Together with the increased oxygen consumption (Supplementary Fig. 5c), the stable energy charge indicates preserved mitochondrial function after supercooling preservation.

The higher metabolic rate during normothermic reperfusion resulted in increased liver function, reflected by bile and urea production and lactate metabolism. Bile (Fig. 3b) production increased as compared to SNMP and the resulting cumulative bile production volumes (per liver weight) correspond to the range of values reported in literature during NMP of transplanted^{22,24,25} and non-transplanted^{20–22} livers. Bile pH, HCO₃ and glucose are increasingly acknowledged as important parameters of biliary function during NMP. The mean bile pH (Fig. 3c) and the bile HCO₃⁻ (Fig. 3d) at the end of reperfusion respectively reached and surpassed the suggested criteria for transplantable liver viability^{22,26}. Although the bile glucose concentrations during reperfusion (Fig. 3e) were higher than proposed clinical transplantable criteria, they were the same as reported for research quality livers by others²². Notably, these livers were perfused after much shorter clinically used durations of HP. Urea production (Supplementary Fig 5d) also increased as a result of the increased metabolic rate and was higher than reported by others during NMP in both *ex vivo*²⁰ and clinical studies²⁷, indicating preserved liver function. Like others during NMP^{16,20,22,24,25}, we observed a rise in lactate during the first hour of reperfusion and subsequent clearance (Fig. 3f and Supplementary Fig. 5e). It should be considered that the livers in this study were initially rejected for transplantation and the confidence intervals of the lactate concentration

at the end of reperfusion largely overlap with time matched values reported by others during NMP of rejected human livers^{20,28}.

In addition to liver function and metabolism we assessed liver injury during simulated transplantation. Absolute values of vascular resistance are dependent on machine perfusion modality and values that correspond to viability remain to be sustained. However, stable resistance profiles as we found during reperfusion (Fig. 3g) are favorable since increasing resistance may reflect endothelial injury and hepatocellular edema as a measure of decreasing viability. The early increase in AST and ALT (Fig. 3h) during the first half hour of reperfusion is less than we expected based on reported AST and ALT levels during NMP in literature^{20–22,24,27}. Histology after reperfusion (Fig. 3 i and j) shows preserved lobular architecture with patches of reversible hepatocellular injury in the form of hepatocellular edema and hydropic changes. Focal spots of hepatocyte dropout with loss of sinusoidal endothelial were observed in the pericentral zone and were markedly correlated to the initial histology of the liver graft, suggesting that the pre-existing injury of the marginal grafts aggravated during reperfusion. We found a significant ($p = 0.009$, $t(2) = 32.89$) increase in apoptotic cells to a percentage of 5.5% (Fig. 3k), while over 15% is normally the case directly after full reperfusion *in vivo* during transplantation²⁹. It should be noted that apoptosis can continue to develop beyond the two-hour time course that is covered by both our *ex vivo* reperfusion model and the peroperative reference during clinical liver transplantation. Limited (hepato)cellular injury is furthermore confirmed by decreasing potassium after the first half our of reperfusion as well (Supplementary Fig. 5f).

In this study, we showed for the first time the feasibility of subzero human organ preservation using discarded human livers. To achieve this, we developed a new multi-temperature perfusion protocol, featuring practical steps to minimize air-liquid interfaces, and repurposed protective agents to stabilize the supercooled state of a large aqueous volume, which was crucial to prevent human livers from freezing during supercooling. We validated our approach with viability assessment of the grafts during SNMP before and after supercooling and by normothermic reperfusion with blood as a model for transplantation. Formally, this model can only suggest the adequacy of supercooling preservation. However, in the case of preclinical human tissue studies, *ex vivo* viability assessment during machine perfusion has strong theoretical background and is supported by experimental and clinical transplantation studies: these all indicate that supercooled human grafts retained their viability despite substantially extended preservation as compared to the clinical standard. Moreover, we observed parameters indicating viability during simulated transplantation of marginal livers up to 44 hours after procurement.

While we limited this feasibility study to -4°C , further optimization of the supercooling protocol could potentially reduce the ice-free storage temperature. Also, reduction or substitution of the glycerol in the supercooling preservation solution might be beneficial to avert potential glycerol phosphorylation during supercooling. Both might lower the rate of ATP depletion during supercooling and consequently increase the preservation duration. Rewarming perfusion is a key step in reducing reperfusion injury after supercooling, and may benefit further from either new machine perfusion modalities used in clinical trials, or emerging approaches in ensuring optimum rewarming temperatures³⁰. The use of human

livers makes this study clinically relevant and promotes the translation of sub-zero organ preservation to the clinic. However, long-term survival experiments of transplanted supercooled livers in swine or an alternative large animal model will be needed before clinical translation.

Online Methods

Organ acquisition

Approval of the institutional review board (IRB) was obtained before any experiments involving the human organs were performed. Human livers were procured in standard fashion¹¹ by the organ procurement organizations (OPO) New England Donor Services Bank (NEDS, Waltham, MA, USA) and LiveOnNY (New York, NY, USA). Informed consent was obtained from the donors by the OPO. After the livers were rejected for transplantation, they were transported to our lab under conventional hypothermic preservation (HP) conditions in University of Wisconsin Solution (UW). We excluded livers based on the following criteria: warm ischemic time >60 min, cold ischemic time >18 hours, >20% macro steatosis, donor history of liver fibrosis and any grade of liver laceration.

Additives for supercooling

Selection of additives to enable supercooled preservation of human livers was informed by our prior studies and literature. 35 kDa PEG and 3-OMG were found to be essential ingredients in our prior rat protocol⁵. As they proved insufficient in scaling up to human livers, we relied on our experience with additives in other biopreservation studies (please note that these prior studies were not supercooling experiments, instead focused on traditional cryopreservation, and other high-subzero approaches that do involve freezing, in various formats). We considered additives including dextrose, glucose, sucrose, DMSO, polyethylene glycol at 8 kDa and 35 kDa, glutathione, vitamin E as well as glycerol and trehalose, based on their hepatotoxicity and post-preservation viability profiles (typically live-dead assay and occasionally ALT release)). Based on these insights we proceeded with glycerol and trehalose for testing in human livers, as detailed in text.

Reagents

Exact composition of the perfusates and storage solution can be found in Supplementary Table 4.. In short, two recovery perfusates ('pre-supercooling recovery solution' and 'post-supercooling recovery solution') were made for sub-normothermic machine perfusion (SNMP) recovery after HP and supercooling. Both were composed of 4 liter modified Williams' medium E (WE) (Sigma Aldrich, St. Louis, MO, USA) and were exactly the same, except the addition of Trolox (Cayman Chemical Company, Ann Arbor, MI, USA) to the post-supercooling recovery solution. For step wise protective agent loading two loading solutions ('loading solution 1' and 'loading solution 2') were made, which respectively composed of 1 and 3 liter of University of Wisconsin solution (UW) (Bridge to Life Ltd., Columbia, SC, USA) supplemented with 35 kDa Polyethylene Glycol (PEG) (Sigma Aldrich, St. Louis, MO, USA), D-(+)-Trehalose dihydrate (Sigma Aldrich, St. Louis, MO, USA) and glycerol (Thermo Fisher Scientific, Waltham, MA, USA). For the stepwise protective agent unloading, 1 liter of modified WE was supplemented with PEG, trehalose

and glycerol. For blood reperfusion, 3 units of non-leuko reduced type O Rh+ packed red blood cells (Research Blood Components LLC, Boston, MA, USA) were combined with 3 units of non-leuko reduced type O Rh+ fresh frozen plasma (Research Blood Components LLC, Boston, MA, USA) and supplemented with modified WE to a total volume of 4 liters. The perfusates were refrigerated at 4°C and the blood was warmed to 37°C before use. The pH of all solutions was corrected to a pH between 7.3–7.4, by addition of NaHCO₃ before priming the perfusion system.

Machine perfusion and supercooling system

The machine perfusion system consists of a duplex non-pulsatile circulation, providing portal and arterial perfusion, see Figure 1b. The liver drains freely in a jacketed organ chamber that also serves as perfusate reservoir (Radnoti, Monrovia, CA, USA). For both portal and arterial circulation, the perfusate is pumped by a flow rate controlled roller pump (Cole Palmer, Vernon Hills, IL, USA) through a heat exchanger combined with a hollow fiber oxygenator (LivaNova, London, UK), a jacketed bubble trap (Radnoti, Monrovia, CA, USA), a pressure sensor (Living Systems Instrumentation, Albans City, VT, USA) and sampling port (Cole Palmer, Vernon Hills, IL, USA), which are connected in series with size 24 silicone tubing (Cole Palmer, Vernon Hills, IL, USA). The two membrane oxygenators are persulfated at a combined flow of 2 L/min with a mixture of 95% O₂ and 5% CO₂. Both bubble traps are filled to 25% and therefore also serve as compliance chamber to minimize pressure pulses created by the roller pumps. The system contains a perfusate in and outflow which can be configured to either recirculation perfusion or single-pass perfusion. The liver and perfusate temperature are controlled by a separated warming/cooling circuit. Water or refrigerant is either warmed by a warm water bath (ThermoFisher Scientific, Pittsburgh, PA, USA) or cooled by a chiller (Optitemp, Traverse City, MI, USA) respectively, and pumped through the heat exchangers and the jackets of the bubble traps and the organ chamber. The chiller contains a 75 liter refrigerant basin that also holds the liver during supercooling.

Protocol

While the graft was submerged in ice cold UW, the common bile duct (CBD), hepatic artery (HA) and portal vein (PV) were dissected. Side branches were identified and tied using 2.0 silk sutures. Subsequently, the cystic duct and artery were dissected, tied and cut distally from the suture. Next, the gallbladder and diaphragm were removed. Cannulas were inserted in the CBD, HA, and PV (Organ Assist, Groningen, the Netherlands) and secured in place by 1.0 silk sutures. Lastly, the liver was flushed with 1.5 and 0.5 liters ice cold ringers lactate through the PV and HA respectively, to remove the UW solution. The vasculature was checked for leaks during the flush, which were tied or repaired with 2.0 silk or 5.0 prolene sutures accordingly.

The machine perfusion system was primed with the pre-supercooling recovery solution and the machine perfusion system in- and outflow were configured in single-pass perfusion. The warm water bath was set at 21°C and connected to the cooling/rewarming circuit. The prepared liver was placed in the organ chamber and the cannulas were de-aired and connected to the perfusion system. Perfusion was initiated by starting the pumps at 50 mL/min. The flow rates were manually adjusted to obtain perfusion pressures of 5 mmHg and 60

mmHg for the PV and HA respectively. The bile duct cannula was connected to a collection reservoir and a needle thermocouple (Omega, Biel, Switzerland) was inserted in the right lobe. After 2 liters of perfusate was passed through the liver, the machine perfusion system was configured from the single-pass to recirculation perfusion and the remaining 2 liters recovery solution was recirculated throughout the perfusion. The liver was gradually rewarmed during the first 30 minutes of perfusion. After 90 minutes of perfusion, regular insulin (Massachusetts General Hospital Pharmacy, Boston, MA, USA) and 3-O-Methyl-D-Glucose (Sigma Aldrich, St. Louis, MO, USA) were added to the perfusate. After 150 minutes, the perfusate and liver were gradually cooled to 4°C in 30 min, by connecting the cooling/rewarming circuit to the chiller. Perfusion pressures were lowered to 3mmHg and 30 mmHg during hypothermic machine perfusion (HMP). After gradual cooling, the machine perfusion system was configured into single-pass perfusion and the livers were perfused with 1L loading solution 1, followed by 3L of loading solution 2.

Following preconditioning during HMP, the liver was disconnected from the machine perfusion system and bagged in a Steri-Drape Isolation Bag (3M Healthcare, St. Paul, MN, USA). Before the bag was closed, all air and residual loading solution was removed. The bagged liver was suspended and fully submerged in the chiller basin and supercooling was initiated by setting the chiller temperature to -4°C. The chiller temperature was regularly checked during supercooling. After 20 hours of supercooling, the liver was removed from the chiller basin. To confirm none of the livers froze during supercooling, the livers were visually inspected, and the soft liver tissue manually palpated when they were removed from the bag.

After the liver was removed from the bag it was connected to the machine perfusion system. Post-supercooling SNMP was identical to pre-supercooling machine perfusion except the following points: (1) Hypothermic single-pass perfusion of 1 L unloading solution preceded the single-pass perfusion of 2 L recovery solution. Similar to pre-supercooling SNMP, the start of perfusion with recovery solution was defined as start of perfusion. (2) Perfusion was continued for 180 minutes at 21°C instead of cooling before supercooling after 150 minutes perfusion. (3) The antioxidant Trolox was added to the perfusate. (4) No 3-OMG or insulin were added to the perfusate.

The temperature of the warm water bath was set to from 21°C to 38°C to warm the liver core temperature to 37°C within 15 minutes. Meanwhile, the single-pass perfusion configuration of the perfusion system was used to replace the 2 L recovery solution with 2 L warm blood which was recirculated during 2 hours reperfusion. Target pressures of 5 mmHg and 60 mmHg were used for the PV and HA respectively.

Viability analysis

The livers were weighed before pre-supercooling SNMP and either after post-supercooling SNMP or blood reperfusion. One liver was weighed after both pre-supercooling SNMP and reperfusion (liver 3). HA and PV flow rates and pressures were registered every 30 minutes during perfusions and reperfusion.

Real time perfusate and blood measurements were performed every 30 minutes; pH, pO₂, HCO₃ and lactate were measured in the PV, HA and vena cava (VC) and Na, K, Ca, Cl, glucose and Hb were measured in the perfusate reservoir, using an Istat blood analyzer (Abbot Laboratories, Chicago, IL, USA). Whole blood counts were performed during reperfusion of one liver (liver 5) using a Cell Dyn Emerald Hematology Analyzer (Abbot Laboratories, Chicago, IL, USA). Every 30 minutes additional 5 mL perfusate samples or plasma samples were collected, immediately frozen on dry ice and stored at -80°C for post hoc analysis of AST, ALT and Urea, using colorimetric kits (ThermoFisher Scientific, Pittsburgh, PA) according to the manufacturers' instructions.

Bile volume in the bile reservoir was measured and collected at the start, mid and end of SNMP and blood reperfusion.

Bilateral wedge biopsies were taken right before and at the end of SNMP and halfway and at the end of blood reperfusion. Biopsies were fixed in buffered 5% formaldehyde for 24 hours and stored in 70% ethanol until outsourced processing and staining for hematoxylin and eosin (HE) and terminal deoxynucleotidyl transferase dUTP nick end labeling (TUNEL) staining (Massachusetts General Hospital Histology Molecular Pathology Core, Boston, MA, USA). HE stained slides were blindly assessed by an experienced liver pathologist (E.O.A.H). Processed TUNEL slides were scanned under 40x magnification using an Aperio ImageScope (Leica Biosystems, Buffalo Grove, IL, USA). For quantification of TUNEL histology, positive cells were counted at 3 square 450 µm sections per slide on standardized locations (at 50% on the radius from the center to the edge of the slide at 0° 60° and 120°) by two independent and blinded measurers. Sections of the wedge biopsies (approx. 1 g) were flash frozen in liquid nitrogen and stored at -80°C. Adenylate triphosphate (ATP), Adenylate diphosphate (ADP), Adenylate monophosphate (AMP), Nicotinamide adenine dinucleotide (NAD⁺ and NADH) were determined as described elsewhere¹². In short, the tissue was homogenized in liquid nitrogen and analysed with targeted multiple reaction monitoring on a 3200 Triple quadrupole liquid chromatography-mass spectrometry system (AB Sciex, Foster City, CA).

To measure the solution melting point, a thin (0.2 mm wire diameter) K-type thermocouple wire (Omega, Biel, Switzerland) was inserted together with the sample in a glass capillary (2.0 mm diameter). The sample was flash frozen and thawed at constant ambient temperature (4°C) while the temperature was logged at 100 ms intervals using a USB Thermocouple Data Acquisition Module (Omega) and Picolog 6 (Picotech, St. Neots, United Kingdom) software. The melting point was derived from the horizontal asymptote of the melting temperature profile.

To measure the melting point of the livers, flash frozen tissue biopsies taken before pre- and post-supercooling SNMP were used. The tissue was crushed in liquid nitrogen and loaded in the glass capillary. The melting point was measured following the same procedure as described for the solutions.

Data processing

To calculate vascular resistance, the perfusion pressure was divided by the corresponding flow rate and initial liver weight.

Energy Charge was calculated with the following formula:

$$\text{ATP} + 0.5\text{ADP} / (\text{ATP} + \text{ADP} + \text{AMP}).$$

Oxygen consumption was calculated with the following formula:

$$\frac{(aO_2 * (\text{art_pO}_2 * \text{art_flow} + \text{Port_pO}_2 * \text{port_flow} - \text{ven_pO}_2 * (\text{art_flow} + \text{port_flow})) + \text{Hb} / 100 * \text{cHb} * (\text{art_sO}_2 / 100 * \text{art_flow} + \text{port_sO}_2 / 100 * \text{port_flow} - \text{ven_sO}_2 / 100 * (\text{art_flow} + \text{port_flow})))}{\text{liver_weight}}.$$

Where aO_2 = oxygen solubility coefficient ($3.14 * 10^{-5}$ mlO₂/mmHgO₂/ml); art_pO_2 = arterial partial oxygen pressure (mmHg); port_pO_2 = portal partial oxygen pressure (mmHg); ven_pO_2 = venous partial oxygen pressure (mmHg); art_flow = arterial flowrate (ml/min); port_flow = portal flowrate (ml/min); art_sO_2 = arterial hemoglobin saturation (%); port_sO_2 = portal hemoglobin saturation (%); ven_sO_2 = venous hemoglobin saturation (%); cHb = hemoglobin oxygen-binding capacity (1.34 mlO₂/gram); Hb = hemoglobin (g/dl); liver_weight = liver weight (kg).

Lactate clearance was calculated with the following formula:

$$\text{art_lactate} * \text{art_flow} + \text{port_lactate} * \text{port_flow} - \text{ven_lactate} * (\text{art_flow} + \text{port_flow}).$$

Where art_lactate = arterial lactate concentration (mM); port_lactate = portal lactate concentration (mM); ven_lactate = venous lactate concentration (mM).

In one case (liver 1), missing portal blood gas values were replaced by the arterial values to calculate oxygen uptake and lactate clearance.

Statistical analyses

Statistical analysis was performed in Prism 7.03 (GraphPad Software Inc., La Jolla, CA). Pre- and post-supercooling SNMP data ($n = 5$) and reperfusion data ($n = 3$) were obtained during independent supercooling experiments using 5 unique human livers (Supplementary Table 2). Data were analyzed for normal distribution by visual inspection and the Shapiro-Wilk normality test. Repeated measures two-way ANOVA, with the Sidak multiple comparisons test, was used for comparison of the time-course perfusion data. The percentages of TUNEL positive cells at the start and end of reperfusion were compared with paired two-tailed student's t tests. Total oxygen consumption was calculated by area under the curve (AUC) analysis and compared with two-tailed student's t tests. The melting points of liver tissues (obtained during the $n = 5$ independent supercooling experiments) and solutions were compared using paired and non-paired two-tailed student's t tests, respectively. The effect sizes of significant differences (η^2) were calculated in Office Excel (Microsoft, Redmont, WA) using the statistical output from prism. P values smaller than

0.05 were considered statistically significant. The summary statistics (F and t values) are provided in text, accompanied by the corresponding degrees freedom in parenthesis.

Data availability

The authors declare that the data supporting the findings of this study are available within the paper and its supplementary information files. Any additional data if needed will be provided upon request.

Reporting Summary

Further information on research design is available in the Nature Research Reporting Summary linked to this article.

Supplementary Material

Refer to Web version on PubMed Central for supplementary material.

Acknowledgements

Funding from the US National Institutes of Health (R01DK096075, R01DK107875 and R01DK114506), and the Department of Defense RTRP W81XWH-17-1-0680 are gratefully acknowledged. We thank Sylvatica Biotech, Inc. and support through the NIH (R21EB023031) and Department of Defense (DHP SBIR H151-013-0141). R.J.V. acknowledges a stipend from the Michael van Vloten Fund for Surgical Research. S.N.T. acknowledges support from NIH K99 HL143149. We thank M. Karabacak, Y.M. Yu and F. Lin at the Mass Spectrometry Core Facility (Shriners Hospital for Children, Boston, Massachusetts) for assistance with adenylate quantification. We thank L. Burlage, A. Matton, B. Bruinsma and C. Pendexter for experimental assistance. Finally, appreciation is extended to LiveON NY, and we are especially grateful for our collaboration with New England Donor Services (NEDS) and their generous support that enables research with human donor organs.

References

1. Giwa S et al. The promise of organ and tissue preservation to transform medicine. *Nat. Biotechnol* 35, 530–542 (2017). [PubMed: 28591112]
2. Buying time for transplants. *Nat. Biotechnol* 35, 801 (2017). [PubMed: 28898224]
3. Bruinsma BG & Uygun K Subzero organ preservation: the dawn of a new ice age? *Curr. Opin. Organ Transplant* 22, 281–286 (2017). [PubMed: 28266941]
4. Berendsen TA et al. Supercooling enables long-term transplantation survival following 4 days of liver preservation. *Nat. Med* 20, 790–793 (2014). [PubMed: 24973919]
5. Bruinsma BG et al. Supercooling preservation and transplantation of the rat liver. *Nat. Protoc* 10, 484–494 (2015). [PubMed: 25692985]
6. Huang H, Yarmush ML & Usta OB Long-term deep-supercooling of large-volume water and red cell suspensions via surface sealing with immiscible liquids. *Nat. Commun* 9, 3201 (2018). [PubMed: 30097570]
7. Storey KB & Storey JM Molecular Biology of Freezing Tolerance in *Comprehensive Physiology* 3, 1283–1308 (American Cancer Society).
8. Dutheil D, Underhaug Gjerde A, Petit-Paris I, Mauco G & Holmsen H Polyethylene glycols interact with membrane glycerophospholipids: is this part of their mechanism for hypothermic graft protection? *J. Chem. Biol* 2, 39–49 (2009). [PubMed: 19568791]
9. Jacobsen IA, Pegg DE, Wusteman MC & Robinson SM Transplantation of rabbit kidneys perfused with glycerol solutions at 10 degrees C. *Cryobiology* 15, 18–26 (1978). [PubMed: 342198]
10. 't Hart NA et al. Determination of an adequate perfusion pressure for continuous dual vessel hypothermic machine perfusion of the rat liver. *Transpl. Int* 20, 343–352 (2007). [PubMed: 17326775]

11. Bruinsma BG et al. Subnormothermic Machine Perfusion for Ex Vivo Preservation and Recovery of the Human Liver for Transplantation: Subnormothermic Machine Perfusion of Human Livers. *Am. J. Transplant* 14, 1400–1409 (2014). [PubMed: 24758155]
12. Bruinsma BG et al. Metabolic profiling during ex vivo machine perfusion of the human liver. *Sci. Rep* 6, 22415 (2016). [PubMed: 26935866]
13. Sridharan GV et al. Metabolomic Modularity Analysis (MMA) to Quantify Human Liver Perfusion Dynamics. *Metabolites* 7, (2017).
14. Vajdová K, Graf R & Clavien P-A ATP-supplies in the cold-preserved liver: A long-neglected factor of organ viability. *Hepatology* 36, 1543–1552 (2002).
15. Higashi H, Takenaka K, Fukuzawa K, Yoshida Y & Sugimachi K Restoration of ATP contents in the transplanted liver closely relates to graft viability in dogs. *Eur. Surg. Res. Eur. Chir. Forsch. Rech. Chir. Eur* 21, 76–82 (1989).
16. Bruinsma BG et al. Peritransplant Energy Changes and Their Correlation to Outcome After Human Liver Transplantation: Transplantation 101, 1637–1644 (2017). [PubMed: 28230641]
17. Lanir A et al. Hepatic transplantation survival: correlation with adenine nucleotide level in donor liver. *Hepatology* 8, 471–475 (1988).
18. Kamiike W et al. Adenine nucleotide metabolism and its relation to organ viability in human liver transplantation. *Transplantation* 45, 138–143 (1988). [PubMed: 3276042]
19. Bruinsma BG, Berendsen TA, Izamis M-L, Yarmush ML & Uygun K Determination and extension of the limits to static cold storage using subnormothermic machine perfusion. *Int. J. Artif. Organs* 36, 775–780 (2013). [PubMed: 24338652]
20. op den Dries S et al. Ex vivo Normothermic Machine Perfusion and Viability Testing of Discarded Human Donor Livers: Normothermic Perfusion of Human Livers. *Am. J. Transplant* 13, 1327–1335 (2013). [PubMed: 23463950]
21. Sutton ME et al. Criteria for viability assessment of discarded human donor livers during ex vivo normothermic machine perfusion. *PloS One* 9, e110642 (2014). [PubMed: 25369327]
22. Watson CJE et al. Observations on the ex situ perfusion of livers for transplantation. *Am. J. Transplant. Off. J. Am. Soc. Transplant. Am. Soc. Transpl. Surg* (2018). doi:10.1111/ajt.14687
23. Avruch JH et al. A novel model for ex situ reperfusion of the human liver following subnormothermic machine perfusion. *TECHNOLOGY* 05, 196–200 (2017).
24. Bral M et al. Preliminary Single-Center Canadian Experience of Human Normothermic Ex Vivo Liver Perfusion: Results of a Clinical Trial. *Am. J. Transplant* 17, 1071–1080 (2017).
25. Mergental H et al. Transplantation of Declined Liver Allografts Following Normothermic Ex-Situ Evaluation. *Am. J. Transplant. Off. J. Am. Soc. Transplant. Am. Soc. Transpl. Surg* 16, 3235–3245 (2016).
26. Matton APM et al. Biliary Bicarbonate, pH and Glucose Are Suitable Biomarkers of Biliary Viability During Ex Situ Normothermic Machine Perfusion of Human Donor Livers. *Transplantation* (2018). doi:10.1097/TP.0000000000002500
27. Reiling J et al. Urea production during normothermic machine perfusion: Price of success? *Liver Transplant. Off. Publ. Am. Assoc. Study Liver Dis. Int. Liver Transplant. Soc* 21, 700–703 (2015).
28. Westerkamp AC et al. Oxygenated Hypothermic Machine Perfusion After Static Cold Storage Improves Hepatobiliary Function of Extended Criteria Donor Livers. *Transplantation* 100, 825–835 (2016). [PubMed: 26863473]
29. Borghi-Scoazec G et al. Apoptosis after ischemia-reperfusion in human liver allografts. *Liver Transplant. Surg. Off. Publ. Am. Assoc. Study Liver Dis. Int. Liver Transplant. Soc* 3, 407–415 (1997).
30. Manuchehrabadi N et al. Improved tissue cryopreservation using inductive heating of magnetic nanoparticles. *Sci. Transl. Med* 9, (2017).

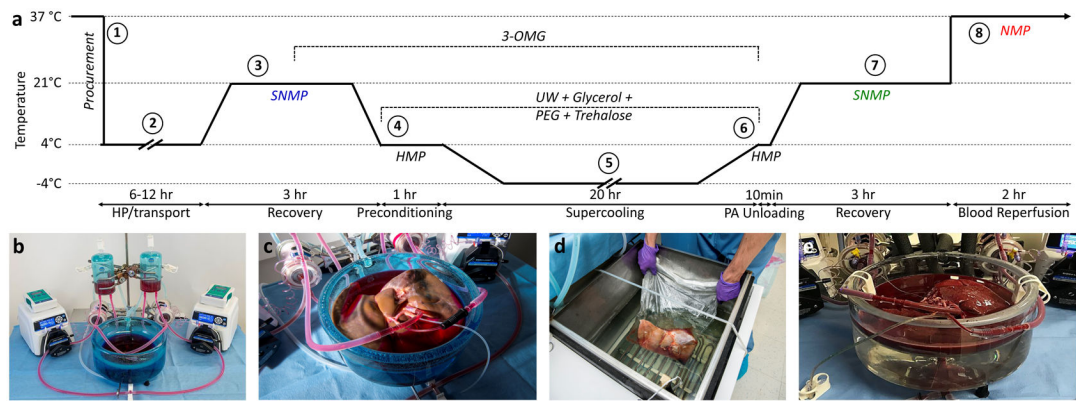


Figure 1. Outline of research design

(a) Schematic temperature profile of the supercooling protocol: The overall research design, entails 8 steps. 1) Five human livers, rejected for transplantation, were procured in standard fashion and 2) transported under hypothermic preservation (HP) conditions. 3) Upon arrival, we recovered the grafts from the incurred warm and cold ischemia and collected pre-supercooling viability parameters during 3 hours of subnormothermic machine perfusion (SNMP). We supplemented the perfusate with 19.42 g/L (200 mM) 3-O-methyl-d-glucose (3-OMG) during the last hour of perfusion. 4) At the end of SNMP, we gradually lowered the perfusion temperature, which was followed by hypothermic machine perfusion (HMP) with University of Wisconsin solution (UW) supplemented with 50 g/L (1.43 μM) 35kD polyethylene glycol (PEG), 37.83 g/L (100 mM) trehalose dihydrate and 125.7 g/L (1.36 M) glycerol. 5) Following preconditioning with the protective agents, the livers were supercooled and stored free of ice at -4°C for 20 hours. 6) After supercooling, the protective agents were gradually washed out, and 7) the livers were recovered by SNMP, identical to pre-supercooling conditions except addition of Trolox to the perfusate and absence of 3-OMG and cooling at the end of SNMP. Post-supercooling viability parameters were collected during SNMP and compared to their baseline values. 8) Three livers were additionally reperfused with non-leukoreduced red blood cells and plasma at 37°C as a model for transplantation. (b) Machine perfusion system. (c) Liver during SNMP recovery. (d) Liver in supercooling basin of the chiller. (e) Normothermic reperfusion with blood of the supercooled liver.

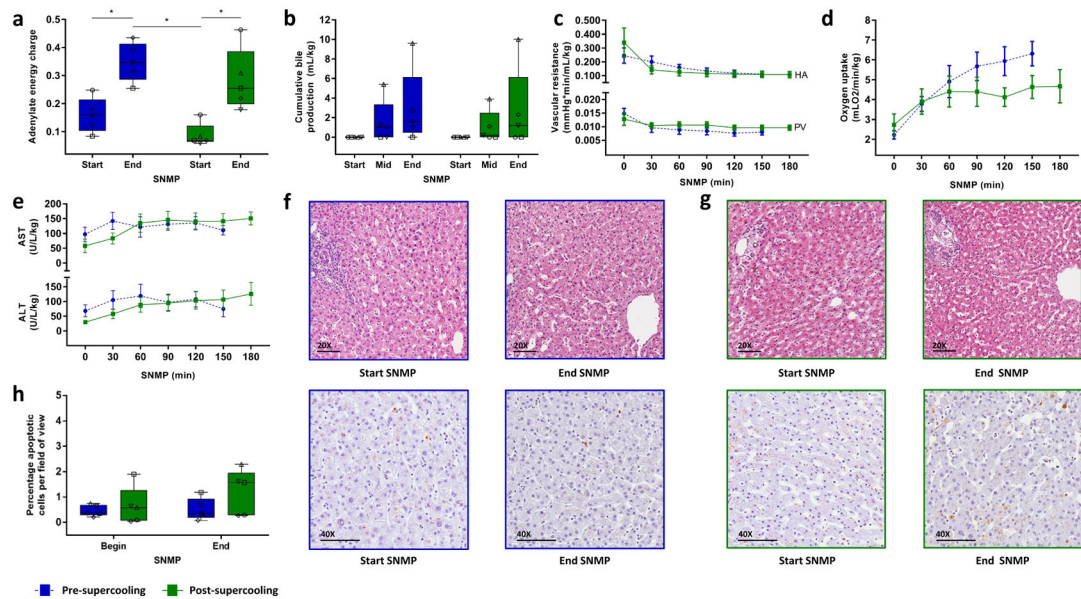


Figure 2. Key *ex vivo* viability parameters and histology during pre- and post-supercooling subnormothermic machine perfusion (SNMP).

(a) Tissue adenylate energy charge showing recovery of energy charge after supercooling. Blue denotes pre-supercooling and green denotes post-supercooling throughout the figure. The symbols of the dot plot overlay correspond to the unique independent biological replicates ($n = 5$ throughout the figure) and match the other (supplementary) figures and tables. (b) Cumulative bile production, also indicating full recovery and identical production after supercooling. (c) Vascular resistance of the hepatic artery (HA) and the portal vein (PV), top and below respectively, indicating no additional resistance in supercooled livers. (d) Oxygen uptake rises and stabilizes similarly. (e) Aspartate AminoTransferase (AST) and Alanine AminoTransferase (ALT) concentrations in the perfusate, top and below respectively, are effectively identical before and after supercooling, indicating no major cellular injury due to preservation. (f) Light microscopy images of parenchymal liver biopsies during pre-supercooling SNMP. Top, hematoxylin and eosin staining (HE). Bottom, staining for apoptotic DNA fragmentation by terminal deoxynucleotidyl transferase dUTP nick end labeling (TUNEL). (g) Light microscopy images of HE (top) and TUNEL (below) stained parenchymal liver biopsies during post-supercooling SNMP. (h) Quantification of TUNEL stained liver biopsies. Apoptotic cells were quantified per field of view of approximately 430 cells. There is a slight but not statistically significant increase in apoptotic cells during SNMP, which is similar before or after supercooled preservation. Stars denote statistical significance ($p < 0.05$, repeated measures two-way ANOVA followed by the Sidak multiple comparisons test). Boxes: median and IQR. Whiskers: min and max. Error bars of line graphs: mean \pm SEM. Scale bars: 100 μm .

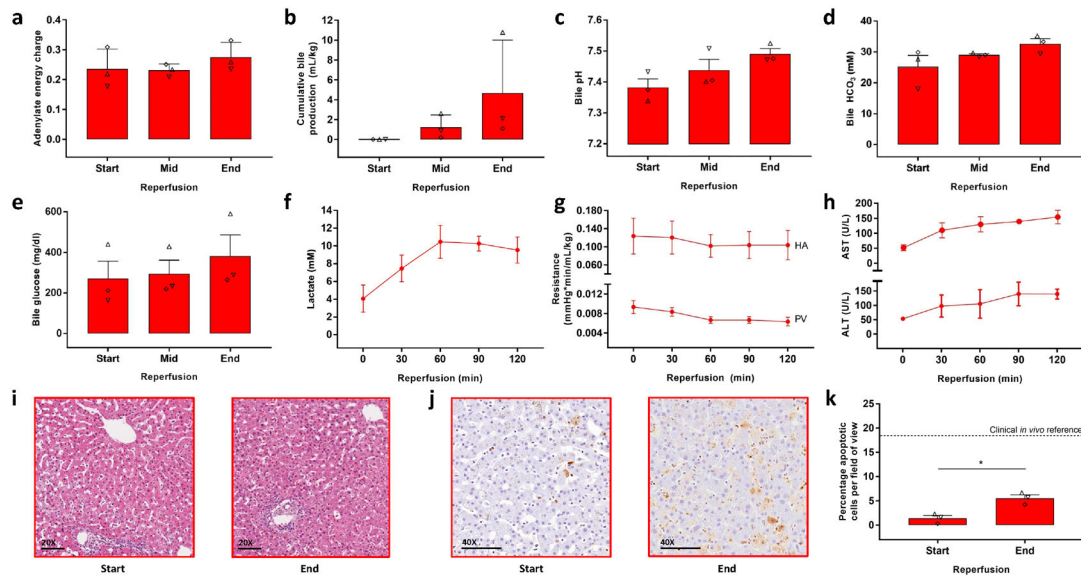


Figure 3. Key *ex vivo* viability parameters during simulated transplantation by normothermic blood reperfusion.

(a) Tissue adenylate energy charge at the start (T = 0 min), mid (T = 60 min) and end (T = 120 min) of reperfusion. The symbols of the dot plot overlay correspond to the unique independent biological replicates (n = 3 throughout the figure) and match the other (supplementary) figures and tables. (b) Cumulative bile production. (c) Bile pH. (d) Bile HCO₃⁻ Concentration. (e) Bile glucose concentration. (f) Lactate concentrations of the arterial inflow. (g) Vascular resistance of the hepatic artery (HA) and the portal vein (PV), top and below respectively. (h) Aspartate AminoTransferase (AST) and Alanine AminoTransferase (ALT) concentrations in the plasma, top and below respectively. (i) Light microscopy images of parenchymal liver biopsies during reperfusion stained with hematoxylin and eosin (HE). (j) Light microscopy images of parenchymal liver biopsies during reperfusion stained for apoptotic DNA fragmentation by terminal deoxynucleotidyl transferase dUTP nick end labeling (TUNEL). (k) Quantification of TUNEL stained liver biopsies. Apoptotic cells were quantified per field of view of approximately 430 cells. The horizontal dashed line represents the reported range of TUNEL positive cells in biopsied taken directly after full reperfusion *in vivo* during liver transplantation²⁹. Star denotes statistical significance ($p = 0.009$, paired two-tailed student's *t* test). Error bars: mean \pm SEM. Scale bars: 100 μ m